



(barium and indium phosphide) and analyzed its crystalline structure. According to [1], both compounds  $\text{Ba}_2\text{P}_7\text{Br}$  and  $\text{Ba}_2\text{P}_7\text{I}$  are crystallized in a new type of monoclinic structure in space group  $P2_1/m$  (No. 11) and are isostructural to  $\text{Ba}_2\text{P}_7\text{Cl}$  [1]. The crystal structures of  $\text{Ba}_2\text{P}_7\text{X}$  ( $X = \text{Cl}, \text{Br}, \text{I}$ ) exhibit the presence of  $\text{P}_7^{-3}$  groups with halogenated anions and barium cations.

Authors think that neither theoretical nor experimental studies of the elastic properties had been carried out. Therefore, such calculations are made in the present work with the inclusion of pressure effects. The results reported in this paper may be useful for evaluating the potential technological applications of  $\text{Ba}_2\text{P}_7\text{X}$ . Knowledge of the elastic constants of crystalline materials is essential to understand many of their basic physical properties. In particular, these constants provide information on the stability and stiffness of the material against externally applied stresses [8]. Knowledge of the pressure dependence of elastic constants and lattice parameters is significant for many modern technologies [8, 9].

## 2. Computational details

Currently, there are different theoretical calculation codes with different approximations. In our calculations, we use the code CASTEP (CambridgeSerial Total Energy Package) [10] which is a direct application of the calculation. All calculations were performed using pseudo-potential plane wave *ab initio* (PP-PW) method based on the density function (DFT). To determine the structural parameters and elastic moduli of the considered compounds, there was used a new version of the generalized gradient approximation (GGA), namely the GGA-PBEsol [11], which has been developed specifically to improve the description of the exchange-correlation in solids. In all electronic total energy calculations, an ultra-soft Vanderbilt pseudo-potential [12] was used to treat the potential seen by the valence electrons due to the nucleus and electrons of the frozen nucleus. Ba  $5s^2 5p^6 6s^2$ , P  $3s^2 3p^3$  and X (Cl  $3s^2 3p^5$ , Br  $4s^2 4p^5$ , I  $5s^2 5p^6 6s^2$ ) have been explicitly treated as valence electron states. Valence's electronic wave functions were extended into a set of truncated plane wave bases at maximum plane energy (cutoff energy) of 380 eV. The Brillouin zone (BZ) was sampled on a  $3 \times 5 \times 5$  Monkhorst-Pack special  $k$  mesh [13]. For  $k$ -points were chosen, after a convergence test, in order to ensure sufficiently accurate calculations.

The fully optimized geometry was carried out with the herein mentioned convergence criteria: (i) the difference of total energy between two consecutive iterations was smaller than  $7.57 \times 10^{-7}$  eV/atom, (ii) maximum force on any atom was smaller than  $0.015$  eV/Å, (iii) stress was smaller than  $0.04$  GPa and (iv) atomic displacement was smaller than  $0.002$  Å. The single-crystal elastic constants  $C_{ij}$  were determined via a linear fitting of the stress-strain curves obtained from first-principles calculations [10]. The elastic constants were done following the convergence of these criteria:  $5.37 \times 10^{-7}$  eV/atom for total energy,  $0.0084$  eV/Å for Hellman-Feynman force and  $3.54 \times 10^{-6}$  Å for maximal ionic displacement. The polycrystalline aggregate elastic moduli, namely the bulk modulus  $B$  and shear modulus  $G$ , were evaluated via the Voigt-Reuss-Hill approximations [14, 15].

## 3. Results and discussions

### 3.1. Structural properties

The ternary semiconductor compounds  $\text{Ba}_2\text{P}_7\text{X}$  where ( $X = \text{Cl}, \text{Br}, \text{I}$ ) have a monoclinic structure and belongs to the  $P2_1/m$  (No. 11), with two inequivalent atomic positions for the barium  $\text{Ba}_1$  and  $\text{Ba}_2$ , and five inequivalent atomic positions for the phosphorous atoms  $\text{P}_1$ ,  $\text{P}_2$ ,  $\text{P}_3$ ,  $\text{P}_4$  and  $\text{P}_5$ . One conventional cell of the  $\text{Ba}_2\text{P}_7\text{Cl}$  crystal is depicted in figure 1.

The conventional cell of  $\text{Ba}_2\text{P}_7\text{X}$  ( $X = \text{Cl}, \text{Br}, \text{I}$ ) contains 20 atoms, 4Ba, 14P and 2X ( $X = \text{Cl}, \text{Br}, \text{I}$ ), which means that the unit cell of  $\text{Ba}_2\text{P}_7\text{X}$  contains two unit formulas ( $Z=2$ ). The atomic positions are  $\text{Ba}_1$ :  $2e(X_{\text{Ba}_1}, 0.25, Z_{\text{Ba}_1})$ ,  $\text{Ba}_2$ :  $2e(X_{\text{Ba}_2}, 0.25, Z_{\text{Ba}_2})$ ,  $\text{P}_1$ :  $2e(X_{\text{P}_1}, 0.25, Z_{\text{P}_1})$ ,  $\text{P}_2$ :  $2e(X_{\text{P}_2}, 0.25, Z_{\text{P}_2})$ ,  $\text{P}_3$ :  $2e(X_{\text{P}_3}, 0.25, Z_{\text{P}_3})$ ,  $\text{P}_4$ :  $4f(X_{\text{P}_4}, Y_{\text{P}_4}, Z_{\text{P}_4})$ ,  $\text{P}_5$ :  $4f(X_{\text{P}_5}, Y_{\text{P}_5}, Z_{\text{P}_5})$  and X:  $2e(X_X, 0.25, Z_X)$ . The atoms are indexed in order to distinguish between the inequivalent crystallographic positions of the same chemical element. Thus, the crystalline structures of the title compounds are characterized by 22 parameters not fixed by the group symmetry, 18 atomic coordinates and three lattice parameters constants ( $a$ ,  $b$  and  $c$ ), one angle  $\beta$ .

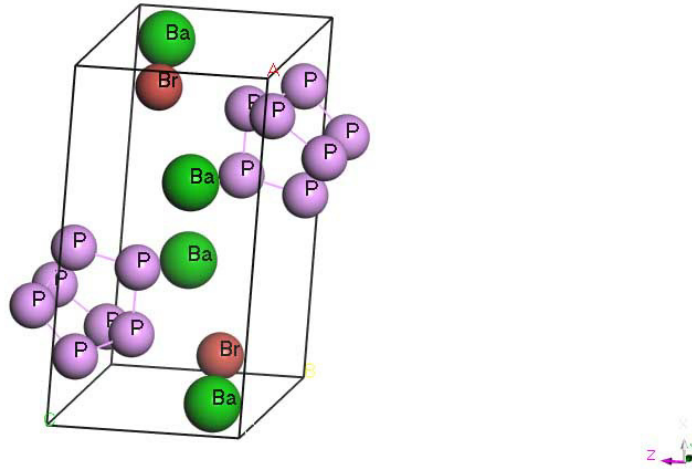


**Figure 1.** (Colour online) The unit-cell crystalline structure of the monoclinic Zintl phase Ba<sub>2</sub>P<sub>7</sub>Br compound.

We have used the experiment lattice constant to start calculating the parameters of the lattice ( $a$ ,  $b$  and  $c$ ), the angle  $\beta$  and the internal atomic coordinates. The calculated equilibrium crystal parameters for Ba<sub>2</sub>P<sub>7</sub>X are presented in table 1 and table 2 along with the available experimental data [16] for the sake of comparison. One can observe an excellent agreement between the calculated and experimental values of the parameters of the lattice ( $a$ ,  $b$  and  $c$ ) and the angle  $\beta$ , the maximum relative difference between the calculated values and their corresponding measured values is very small. In addition, the calculated and the measured atomic internal coordinates of all atoms of the unit cell match each other well. This excellent matching serves as a proof of the reliability and accuracy of the chosen calculation method and provides confidence in the results of the following calculations of the structural and elastic properties of the considered system.

We note that the unit cell volume of Ba<sub>2</sub>P<sub>7</sub>I is wider than that of Ba<sub>2</sub>P<sub>7</sub>Br which is larger than that of Ba<sub>2</sub>P<sub>7</sub>Cl, which can be attributed to the fact that the I atom radius is larger than that Br than that greater than that of Cl atom, i.e., the unit-cell volume of ternary compounds of Zintl type increases when moving down in column VII of the periodic table.

In order to objectively study the chemical and structural stability of the monoclinic ternary Ba<sub>2</sub>P<sub>7</sub>X, the cohesive energy  $E_{\text{coh}}$  and formation enthalpy  $\Delta H$  are calculated using the following expressions [17]:

$$E_{\text{coh}} = \frac{1}{N_{\text{Ba}} + N_{\text{P}} + N_{\text{X}}} \left[ E_{\text{Tot}}^{\text{Ba}_2\text{P}_7\text{X}} - \left( N_{\text{Ba}} E_{\text{Tot}}^{\text{Ba(atom)}} + N_{\text{P}} E_{\text{Tot}}^{\text{P(atom)}} + N_{\text{X}} E_{\text{Tot}}^{\text{X(atom)}} \right) \right]. \quad (3.1)$$

Where these quantities  $E_{\text{Tot}}^{\text{Ba}_2\text{P}_7\text{X}}$ ,  $E_{\text{Tot}}^{\text{Ba(atom)}}$ ,  $E_{\text{Tot}}^{\text{P(atom)}}$  and  $E_{\text{Tot}}^{\text{X(atom)}}$  represent the total energy of the primitive cell of Ba<sub>2</sub>P<sub>7</sub>X and the total energies of the isolated Ba, P and X atoms, respectively.  $N_{\text{Ba}}$ ,  $N_{\text{P}}$  and  $N_{\text{X}}$  are the number of Ba, P and X atoms in the primitive cell, respectively. The energy of the free atom was calculated using a cubic box with a large lattice constant that contained the considered atom. The formation enthalpy  $\Delta H$  of Ba<sub>2</sub>P<sub>7</sub>X was calculated using the following expression [17]:

$$\Delta H = \frac{1}{N_{\text{Ba}} + N_{\text{P}} + N_{\text{X}}} \left[ E_{\text{Tot}}^{\text{Ba}_2\text{P}_7\text{X}} - \left( N_{\text{Ba}} E_{\text{Tot}}^{\text{Ba(solid)}} + N_{\text{P}} E_{\text{Tot}}^{\text{P(solid)}} + N_{\text{X}} E_{\text{Tot}}^{\text{X(solid)}} \right) \right]. \quad (3.2)$$

Here,  $E_{\text{Tot}}^{\text{Ba(solid)}}$ ,  $E_{\text{Tot}}^{\text{P(solid)}}$  and  $E_{\text{Tot}}^{\text{X(solid)}}$  denote the total energies per atom of the solid states of the pure elements Ba, P and X, respectively. The thermodynamic and chemical stabilities of the Ba<sub>2</sub>P<sub>7</sub>Cl, Ba<sub>2</sub>P<sub>7</sub>Br and Ba<sub>2</sub>P<sub>7</sub>I compounds can be judged from their formation enthalpies and cohesive energies. As can be seen from table 1, three considered compounds monoclinic Zintl phase have negative cohesive energies and formation enthalpies, indicating that they are energetically stable.

**Table 1.** The calculated equilibrium crystal lattice constants ( $a$ ,  $b$  and  $c$ , in Å), angle  $\beta$  (in deg), unit-cell volume ( $V$ , in Å<sup>3</sup>), cohesive energy ( $E_{\text{coh}}$ , in eV/atom) and formation enthalpy ( $\Delta H$ , in eV/atom) for the monoclinic Zintl phase Ba<sub>2</sub>P<sub>7</sub>X (X=Cl, Br, I) compared with the available experimental data.

Structural parameter	Ba <sub>2</sub> P <sub>7</sub> Cl		Ba <sub>2</sub> P <sub>7</sub> Br		Ba <sub>2</sub> P <sub>7</sub> I	
	Present work	Expt [16]	Present work	Expt [16]	Present work	Expt [16]
$a$	11.618	11.726	11.786	11.850	11.975	12.0392
$b$	6.731	6.829	6.779	6.835	6.834	6.8990
$c$	6.270	6.337	6.232	6.294	6.292	6.3538
$\beta$	95.350	95.270	95.951	95.819	96.127	95.915
$V$	488.223	505.302	495.309	507.2	6.292	524.93
$E_{\text{coh}}$	-5.53	-	-5.48	-	512.023	-
$\Delta H$	-0.38	-	-0.31	-	-0.280	-

**Table 2.** Optimized atomic coordinates for the monoclinic Zintl Phase Ba<sub>2</sub>P<sub>7</sub>X (X=Cl, Br, I) in comparison with experiment.

		Ba <sub>2</sub> P <sub>7</sub> Cl			Ba <sub>2</sub> P <sub>7</sub> Br			Ba <sub>2</sub> P <sub>7</sub> I		
		$x$	$y$	$z$	$x$	$y$	$z$	$x$	$y$	$z$
Ba <sub>1</sub> (2e)	present	0.0466	0.25	0.229	0.0459	0.25	0.2113	0.05	0.25	0.1968
	Expt [16]	0.045	0.25	0.2292	-	-	-	-	-	-
Ba <sub>1</sub> (2e)	Present	0.6524	0.25	0.4348	0.6469	0.25	0.4343	0.638	0.25	0.4291
	Expt [16]	6524	0.25	0.4332	-	-	-	-	-	-
X (2e)	Present	0.9115	0.25	0.6379	0.9145	0.25	0.6558	0.9142	0.25	0.001
	Expt [16]	0.9113	0.25	0.6366	-	-	-	-	-	-
P <sub>1</sub> (2e)	Present	0.452	0.25	0.0098	0.4501	0.25	0.0067	0.4481	0.25	0.6617
	Expt [16]	0.451	0.25	0.01	-	-	-	-	-	-
P <sub>2</sub> (2e)	Present	0.2212	0.25	0.6764	0.222	0.25	0.6661	0.2234	0.25	0.6609
	Expt [16]	0.2222	0.25	0.6767	-	-	-	-	-	-
P <sub>3</sub> (2e)	Present	0.4076	0.25	0.6696	0.4063	0.25	0.6639	0.405	0.25	0.6609
	Expt [16]	0.408	0.25	0.6722	-	-	-	-	-	-
P <sub>4</sub> (2e)	Present	0.1939	0.4989	0.8834	0.1959	0.4980	0.8763	0.1986	0.0016	0.8662
	Expt [16]	0.1946	0.0047	0.8828	-	-	-	-	-	-
P <sub>5</sub> (2e)	Present	0.3142	0.0768	0.1483	0.3139	0.0784	0.1441	0.3141	0.0797	0.1370
	Expt [16]	0.3141	0.0789	0.1466	-	-	-	-	-	-

The most frequently used methods of testing the reliability of the obtained theoretical results consist in comparing the numerical values of a property obtained by different theoretical procedures. For this problem, the bulk module  $B$  was used as a test parameter. The calculations of the unit-cell volume  $V$  and the total energy  $E_{\text{Tot}}$  of a solid for different values of the pressure  $P$  provide a convenient method for estimating the bulk modulus  $B$  and its pressure derivative  $B'$ . For this purpose, the structural parameters of the test compounds were calculated at fixed applied hydrostatic pressures in the range of 0 to 15 GPa with a pitch of 5 GPa, such an option being implemented in the CASTEP code and makes it possible to find an optimized structure at any axial or hydrostatic pressure, so that the hydrostatic pressure can significantly affect the physical properties of the materials. One of the most obvious manifestations of the effect of the application of hydrostatic pressure to a material is a decrease of its volume and lattice constants. Figure 2 demonstrates the dependence in pressure of the normalized lattice constants ( $a/a_0$ ,  $b/b_0$  and  $c/c_0$ ), the normalized unit-cell volume ( $V/V_0$ ) and the normalized angle  $\beta$  ( $\beta/\beta_0$ ). We have fitted these quantities  $a/a_0$ ,  $b/b_0$ ,  $c/c_0$  and ( $V/V_0$ ) (where  $a_0$ ,  $b_0$ ,  $c_0$  and  $V_0$  are the lattice parameters and unit-cell volume at zero pressure) using a polynomial expression in the following form:

$$\frac{X(P)}{X_0} = 1 + B_X P + \sum_{n=2}^3 K_n P^n, \quad (3.3)$$

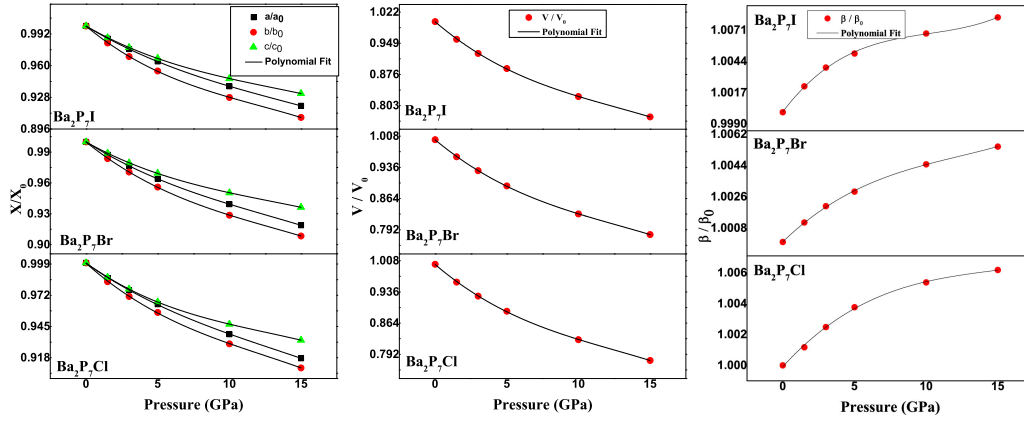


**Figure 2.** (Colour online) Pressure-dependent variations of the lattice constants  $a$ ,  $b$  and  $c$ , the unit-cell volume and the angle  $\beta$  for the monoclinic Zintl phase Ba<sub>2</sub>P<sub>7</sub>X (X=Cl, Br, I). The “0” subscript denotes the value of the parameter at zero pressure.

where  $X = a, b, c, V$ . The obtained linear compressibilities  $B_a$ ,  $B_b$  and  $B_c$  of the lattice parameters  $a$ ,  $b$  and  $c$ , respectively, and the volume compressibility  $B_V$  were used to estimate the bulk modulus  $B$  as follows:

$$B = \frac{1}{B_a + B_b + B_c}, \quad (3.4)$$

$$B = \frac{1}{B_V}. \quad (3.5)$$

We observe a third-order polynomial dependence in all curves as the pressure increases from 0 GPa to 15 GPa. Cellular axes and volume decrease with pressure while  $B/B_0$  increases. Moreover, we can see that the ratio  $b/b_0$  decreases more rapidly than  $a/a_0$  and  $c/c_0$  in the three materials, respectively, which indicates that the axis  $b$  is much more compressible than the axes  $a$  and  $c$ . The deduced values of compressibility  $Bx = -\frac{1}{x} \frac{dx}{dP}$ . From the fit, for the three materials Ba<sub>2</sub>P<sub>7</sub>X (X = Cl, Br, I), respectively. The following relations were obtained from these calculations:

for the Ba<sub>2</sub>P<sub>7</sub>Cl:

$B_a = 0.00885 \text{ GPa}^{-1}$ ,  $B_b = 0.01102 \text{ GPa}^{-1}$ ,  $B_c = 0.00888 \text{ GPa}^{-1}$  and  $B_V = 0.02831 \text{ GPa}^{-1}$ . The obtained polynomials the fit are:

$$\begin{cases} \frac{a}{a_0} &= 1 - 0.00885P + 3.38214 \times 10^{-4}P^2 - 8.45661 \times 10^{-6}P^3, \\ \frac{b}{b_0} &= 1 - 0.01102P + 5.57587 \times 10^{-4}P^2 - 1.5016 \times 10^{-5}P^3, \\ \frac{c}{c_0} &= 1 - 0.00888P + 4.88156 \times 10^{-4}P^2 - 1.28474 \times 10^{-5}P^3, \\ \frac{V}{V_0} &= 1 - 0.02831P + 1.15 \times 10^{-3}P^2 - 3.97585 \times 10^{-5}P^3, \\ \frac{\beta}{\beta_0} &= 1 + 1.02 \times 10^{-3}P - 6.0406 \times 10^{-5}P^2 + 1.34967 \times 10^{-6}P^3, \end{cases} \quad (3.6)$$

for the Ba<sub>2</sub>P<sub>7</sub>Br:  $B_a = 0.0088 \text{ GPa}^{-1}$ ,  $B_b = 0.01122 \text{ GPa}^{-1}$ ,  $B_c = 0.00782 \text{ GPa}^{-1}$  et  $B_V = 0.02765 \text{ GPa}^{-1}$ . The obtained polynomials the fit are:

$$\begin{cases} \frac{a}{a_0} &= 1 - 0.0088P + 3.704 \times 10^{-4}P^2 - 9.6174 \times 10^{-6}P^3, \\ \frac{b}{b_0} &= 1 - 0.01122P + 5.5058 \times 10^{-4}P^2 - 1.39338 \times 10^{-5}P^3, \\ \frac{c}{c_0} &= 1 - 0.00782P + 3.86272 \times 10^{-4}P^2 - 9.86085 \times 10^{-5}P^3, \\ \frac{V}{V_0} &= 1 - 0.02765P + 1.43 \times 10^{-3}P^2 - 3.70713 \times 10^{-5}P^3, \\ \frac{\beta}{\beta_0} &= 1 + 7.95806 \times 10^{-4}P - 4.81896 \times 10^{-5}P^2 + 1.29935 \times 10^{-6}P^3, \end{cases} \quad (3.7)$$

for the Ba<sub>2</sub>P<sub>7</sub>I:  $B_a = 0.00865 \text{ GPa}^{-1}$ ,  $B_b = 0.0119 \text{ GPa}^{-1}$ ,  $B_c = 0.00829 \text{ GPa}^{-1}$  and  $B_V = 0.02879 \text{ GPa}^{-1}$ .

The obtained polynomials the fit are:

$$\left\{ \begin{array}{l} \frac{a}{a_0} = 1 - 0.00865P + 3.38005 \times 10^{-4}P^2 - 7.91834 \times 10^{-6}P^3, \\ \frac{b}{b_0} = 1 - 0.01196P + 6.6066 \times 10^{-4}P^2 - 1.81681 \times 10^{-5}P^3, \\ \frac{c}{c_0} = 1 - 0.00829P + 4.01591 \times 10^{-4}P^2 - 1.00773 \times 10^{-5}P^3, \\ \frac{V}{V_0} = 1 - 0.02879P + 1.53 \times 10^{-3}P^2 - 4.02183 \times 10^{-5}P^3, \\ \frac{\beta}{\beta_0} = 1 + 1.62 \times 10^{-3}P - 1.41829 \times 10^{-4}P^2 + 4.65511 \times 10^{-6}P^3. \end{array} \right. \quad (3.8)$$

When the pressure changes from 0 to 15 GPa, a, b and c decrease approximately 8 %, 9 % and 6 %, respectively, in the three materials Ba<sub>2</sub>P<sub>7</sub>X (X=Cl, Br, I). Consequently, the axis b is the most compressible under external pressure, and the c axis is the least compressible; the effect of the pressure on the axis b is much greater than on the c axis. Thus, Ba<sub>2</sub>P<sub>7</sub>X is anisotropic in compressibility.

In the present work, the pressure versus volume ( $P - V$ ) data were fitted to the Birch Murnaghan [18, 19], Murnaghan  $P - V$  EOS [20], and Vinet exponential equations of state [21] equation of state, and the energy versus volume ( $E_{\text{Tot}} - V$ ) data were fitted to the Birch Murnaghan [22] and Murnaghan equations of state [23]. Figure 3 shows the obtained results from the bulk modulus  $B$  and its pressure derivative  $B'$  is given in table 3. One can appreciate the good agreement between the values of the bulk modulus  $B$  obtained from different procedures, the linear compressibilities ( $B_a$ ,  $B_b$  and  $B_c$ ), the volume compressibility ( $B_V$ ) and the EOSs fits. This constitutes a good proof for the reliability of our calculations. The obtained bulk modulus values in our work will be compared to the corresponding ones that will be achieved from the elastic constants later on.

- a Calculated from GGA PBEsol,
- b Calculated from Hill's approximation,
- c Calculated from Vinet  $P - V$  EOS [21],
- d Calculated from Murnaghan  $P - V$  EOS [20],
- e Calculated from Birch-Murnaghan  $P - V$  EOS [18],
- f Calculated from Murnaghan  $E - V$  EOS [22],
- g Calculated from Birch-Murnaghan  $E - V$  EOS [23],
- h Calculated from linear compressibilities  $B = 1/(B_a + B_b + B_c)$ ,
- i Calculated from the compressibility  $1/B_V$ .

## 3.2. Elastic properties

### 3.2.1. Single-crystal elastic constants

Elastic constants  $C_{ijs}$  of materials are important parameters because they provide information on their response when a stress is applied to the material [24].

For monoclinic crystals, there are 13 independent elastic constants, namely,  $C_{11}$ ,  $C_{22}$ ,  $C_{33}$ ,  $C_{44}$ ,  $C_{55}$ ,  $C_{66}$ ,  $C_{12}$ ,  $C_{13}$ ,  $C_{15}$ ,  $C_{23}$ ,  $C_{25}$ ,  $C_{35}$  and  $C_{46}$ . When the  $C_{11}$ ,  $C_{22}$  and  $C_{33}$  represent the stiffness of the material when a uniaxial stress is applied along the principal  $X$ ,  $Y$  and  $Z$  axes, respectively.  $C_{44}$  measures the

**Table 3.** Calculated bulk modulus ( $B$ , in GPa) and its pressure derivative  $B'$ .

	Ba <sub>2</sub> P <sub>7</sub> Cl			Ba <sub>2</sub> P <sub>7</sub> Br			Ba <sub>2</sub> P <sub>7</sub> I		
$B$	34.013 <sup>a</sup>	34.014 <sup>b</sup>	32.93 <sup>c</sup>	34.29 <sup>a</sup>	34.75 <sup>b</sup>	33.75 <sup>c</sup>	32.94 <sup>a</sup>	35.2 <sup>b</sup>	32.08 <sup>c</sup>
	33.95 <sup>d</sup>	33.31 <sup>e</sup>	30.87 <sup>f</sup>	34.76 <sup>d</sup>	34.12 <sup>e</sup>	32.19 <sup>f</sup>	33.12 <sup>d</sup>	32.46 <sup>e</sup>	30.21 <sup>f</sup>
	31.26 <sup>g</sup>	34.78 <sup>h</sup>	35.32 <sup>i</sup>	32.46 <sup>g</sup>	35.91 <sup>h</sup>	36.16 <sup>i</sup>	30.68 <sup>g</sup>	34.67 <sup>h</sup>	34.73 <sup>i</sup>
$B'$	4.89 <sup>c</sup>	4.14 <sup>d</sup>	4.61 <sup>e</sup>	4.89 <sup>c</sup>	4.15 <sup>d</sup>	4.61 <sup>e</sup>	5.01 <sup>c</sup>	4.23 <sup>d</sup>	4.73 <sup>e</sup>
	5.16 <sup>f</sup>	5.41 <sup>g</sup>	–	5.00 <sup>f</sup>	5.27 <sup>g</sup>	–	5.23 <sup>f</sup>	5.47 <sup>g</sup>	–

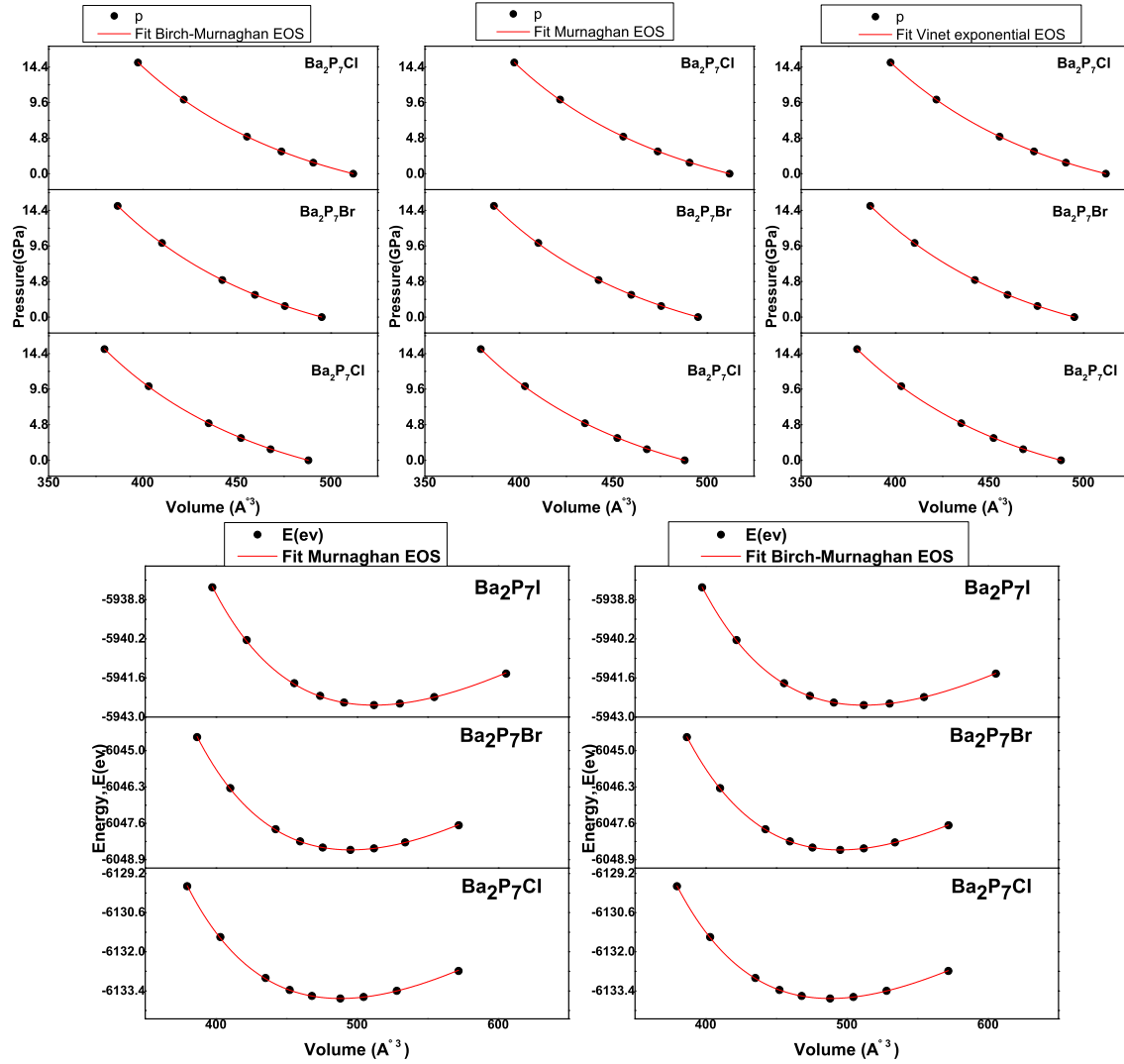


**Figure 3.** (Colour online) Calculated pressure ( $P$ ) and total energy ( $E$ ) versus unit-cell volume  $V$  and fits to Birch-Murnaghan, Murnaghan and Vinet equation of states for the Ba<sub>2</sub>P<sub>7</sub>Cl, Ba<sub>2</sub>P<sub>7</sub>Br and Ba<sub>2</sub>P<sub>7</sub>I compounds.

shear elastic modulus along  $Y$ -axis on  $Z$ -plane;  $C_{55}$  measures the shear elastic modulus along  $Z$ -axis on  $X$ -plane. Thus,  $C_{66}$  represents the shear along  $X$ -axis on the  $Y$ -plane. The complete set of the calculated independent elastic constants  $C_{ij}$ s of the Ba<sub>2</sub>P<sub>7</sub>Cl, Ba<sub>2</sub>P<sub>7</sub>Br and Ba<sub>2</sub>P<sub>7</sub>I compounds. The present work is the first attempt to calculate the elastic constants  $C_{ij}$ s of the title compounds. No experimental or theoretical values for these quantities are reported in the literature, which is why comparison with other results is not possible. From the obtained results, we can make the following conclusions:

(i) The values  $C_{11}$ ,  $C_{22}$  and  $C_{33}$  are noticed to be larger than the ones of  $C_{44}$ ,  $C_{55}$ ,  $C_{66}$ ,  $C_{12}$ ,  $C_{13}$ ,  $C_{15}$ ,  $C_{25}$ ,  $C_{35}$  and  $C_{46}$ , which denotes that the considered system is of a bigger resistance to unidirectional compression than to shear deformation.

(ii) The stiffness-to-uniaxial stress along the crystallographic  $a$ ,  $b$  and  $c$  axes, respectively, is replicated by  $C_{11}$ ,  $C_{22}$  and  $C_{33}$  elastic constants. For three compounds Ba<sub>2</sub>P<sub>7</sub>Cl, Ba<sub>2</sub>P<sub>7</sub>Br and Ba<sub>2</sub>P<sub>7</sub>I, the obtained values for elastic constants  $C_{11}$ ,  $C_{22}$ ,  $C_{33}$  under external pressure of 0 to 15 GPa by 5 GPa step are roughly equal when 0 GPa is pressed, but with an external pressure variation of 0 to 15 GPa, we observe an increase of  $C_{11}$ ,  $C_{22}$  et  $C_{33}$ , with  $C_{22}$  increase of about 64 % compared with  $C_{33}$ ,  $C_{11}$  values, which is an increase by less than 64 % for the three compounds B<sub>2</sub>P<sub>7</sub>X(X=Cl, Br, I) indicating that the three compounds are

relatively more compressible when compressed along the [010] crystallographic directions than along the [100] and [001]. These results agree totally with the results already obtained from the study of the pressure dependence of the lattice parameters.

(iii) To be mechanically stable, the calculated zero-pressure single-crystal elastic constants  $C_{ijs}$  of monoclinic crystals should satisfy the following stability criteria [25]:

$$\left\{ \begin{array}{l} C_{ii} > 0, \quad i = 1, 2, 3, 4, 5, 6, \\ [C_{11} + C_{22} + C_{33} + 2(C_{12} + C_{13} + C_{23})] > 0, \\ (C_{33}C_{55} - C_{35}^2) > 0, \quad (C_{44}C_{66} - C_{46}^2) > 0, \quad (C_{22} + C_{33} - 2C_{23}) > 0, \\ [C_{22}(C_{33}C_{55} - C_{35}^2) + 2C_{23}C_{25}C_{35} - C_{23}^2C_{55} - C_{25}^2C_{33}] > 0, \\ \left\{ \begin{array}{l} 2[C_{15}C_{25}(C_{33}C_{12} - C_{13}C_{23}) + C_{15}C_{35}(C_{22}C_{13} - C_{12}C_{23}) + C_{25}C_{35}(C_{11}C_{23} - C_{12}C_{13})] \\ - [C_{15}^2(C_{22}C_{33} - C_{23}^2) + C_{25}^2(C_{11}C_{33} - C_{13}^2) + C_{35}^2(C_{11}C_{22} - C_{12}^2)] + C_{55}g \end{array} \right\} > 0, \\ g = C_{11}C_{22}C_{33} - C_{11}C_{23}^2 - C_{22}C_{13}^2 - C_{33}C_{12}^2 + C_{12}C_{13}C_{23}. \end{array} \right. \quad (3.9)$$

Thus, we can assert that the monoclinic Zintl phase  $\text{Ba}_2\text{P}_7\text{X}$  is in a mechanically stable state.

(iv) The crystal's mechanical stability at any pressure, which requires strain energy to be positive, is confirmed when the set of elastic constants  $C_{ijs}$  responds to special restrictions. This criterion is fulfilled if a symmetric matrix  $G_{ij}$  is of a positive determinant [26]. The symmetric matrix  $\tilde{G}_{ij}$  for any structure type is defined as follows:

$$\tilde{G} = \begin{vmatrix} \tilde{C}_{11} & \tilde{C}_{12} & \tilde{C}_{13} & 2C_{14} & 2C_{15} & 2C_{16} \\ \tilde{C}_{21} & \tilde{C}_{22} & \tilde{C}_{23} & 2C_{24} & 2C_{25} & 2C_{26} \\ \tilde{C}_{31} & \tilde{C}_{32} & \tilde{C}_{33} & 2C_{34} & 2C_{35} & 2C_{36} \\ 2C_{41} & 2C_{42} & 2C_{43} & 4\tilde{C}_{44} & 4C_{45} & 4C_{46} \\ 2C_{52} & 2C_{52} & 2C_{53} & 4C_{54} & 4\tilde{C}_{55} & 4C_{56} \\ 2C_{61} & 2C_{62} & 2C_{63} & 4C_{64} & 4C_{65} & 4\tilde{C}_{66} \end{vmatrix}. \quad (3.10)$$

Here,  $\tilde{C}_{\alpha\alpha} = C_{\alpha\alpha} - P$ , where  $\alpha = 1, 2, \dots, 6$ , and  $\tilde{C}_{12} = C_{12} + P$ ,  $\tilde{C}_{13} = C_{13} + P$ ,  $\tilde{C}_{23} = C_{23} + P$ . The calculated values for the  $C_{ijs}$  of the monoclinic  $\text{Ba}_2\text{P}_7\text{X}$  ( $\text{X} = \text{Cl}, \text{Br}, \text{I}$ ) compounds in the pressure range of 0–15 GPa obey these conditions well, which means that this compound remains mechanically stable in the considered pressure range.

(v) Figure 4 shows the pressure dependence of the 13 independent elastic constants of the monoclinic compounds for pressures up to 15 GPa. Apart from  $C_{25}$  and  $C_{46}$ , the remainder of the elastic constants  $C_{ij}$  increase monotonously with an increasing pressure but with different sensitivities.  $C_{25}$  and  $C_{46}$  decrease monotonously with an increasing pressure. The lines represent the second-order polynomial fits to the results. The fit results given by the following expressions for the three compounds  $\text{Ba}_2\text{P}_7\text{Cl}$ ,  $\text{Ba}_2\text{P}_7\text{Br}$  and  $\text{Ba}_2\text{P}_7\text{I}$ , respectively, are as follows:

$$\left\{ \begin{array}{l} C_{11} = 64.25 + 6.004P - 0.088P^2, \\ C_{22} = 55.89 + 7.47P - 0.065P^2, \\ C_{33} = 52.53 + 7.98P - 0.12P^2, \\ C_{44} = 19.44 + 1.97P - 0.046P^2, \\ C_{55} = 25.77 + 1.91P - 0.048P^2, \\ C_{66} = 17.86 + 2.12P - 0.036P^2, \end{array} \right\} \left\{ \begin{array}{l} C_{12} = 18.76 + 2.53P - 0.017P^2, \\ C_{13} = 28.32 + 5.17P - 0.075P^2, \\ C_{15} = -0.93 + 0.034P + 0.014P^2, \\ C_{23} = 21.11 + 3.69P - 0.056P^2, \\ C_{25} = -0.70 - 0.10P - 0.0086P^2, \\ C_{35} = -3.43 + 0.32P - 6 \times 10^{-4}P^2, \\ C_{46} = -4.00 - 0.35P - 0.0045P^2, \end{array} \right. \quad (3.11)$$

$$\left\{ \begin{array}{l} C_{11} = 62.62 + 6.75P - 0.10P^2, \\ C_{22} = 57.74 + 7.95P - 0.067P^2, \\ C_{33} = 56.13 + 8.37P - 0.12P^2, \\ C_{44} = 17.94 + 1.90P - 0.05P^2, \\ C_{55} = 26.33 + 2.22P - 0.026P^2, \\ C_{66} = 17.08 + 1.98P - 0.032P^2, \end{array} \right\} \left\{ \begin{array}{l} C_{12} = 18.19 + 2.60P - 0.021P^2, \\ C_{13} = 29.20 + 4.92P - 0.054P^2, \\ C_{15} = -0.15 + 0.189P + 0.014P^2, \\ C_{23} = 19.41 + 3.15P - 0.034P^2, \\ C_{25} = -1.64 - 0.34P - 0.0036P^2, \\ C_{35} = -3.7 - 0.28P - 1.4 \times 10^{-3}P^2, \\ C_{46} = -3.7 - 0.28P - 0.006P^2, \end{array} \right. \quad (3.12)$$



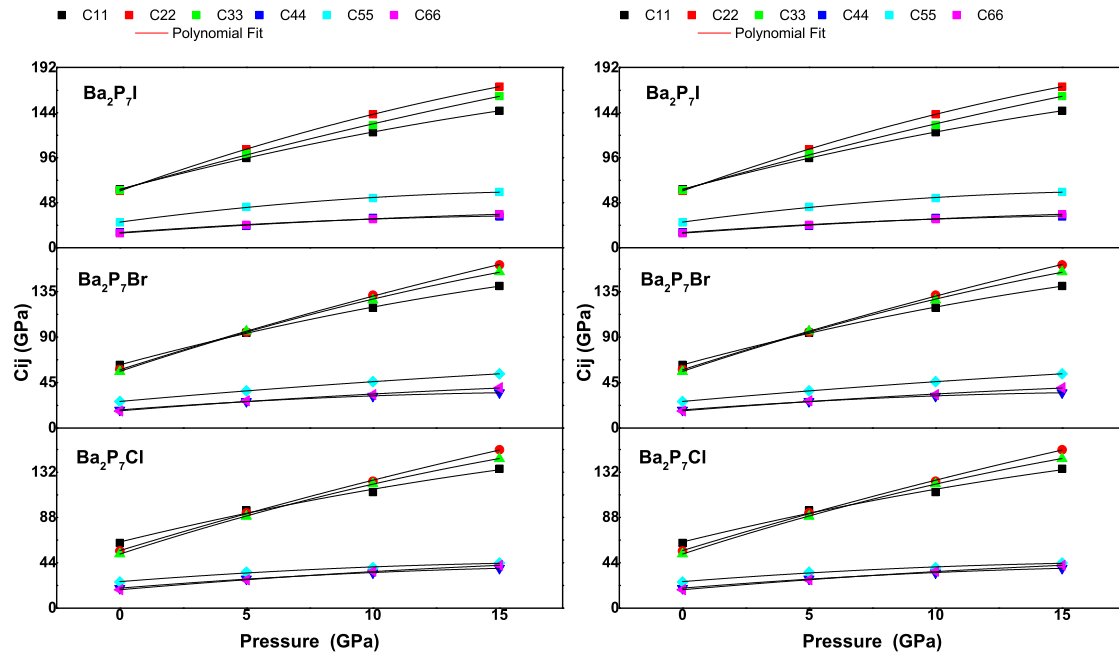


**Figure 4.** (Colour online) The calculated pressure dependence of the independent elastic constants  $C_{ijs}$  of the monoclinic Zintl phase Ba<sub>2</sub>P<sub>7</sub>X. The symbols indicate the calculated results. The lines represent the results of fitting these theoretical results to a second-order polynomial.

$$\left\{ \begin{array}{l} C_{11} = 62.43 + 7.15P - 0.10P^2, \\ C_{22} = 60.63 + 9.68P - 0.15P^2, \\ C_{33} = 62.016 + 7.78P - 0.076P^2, \\ C_{44} = 16.17 + 1.96P - 0.052P^2, \\ C_{55} = 27.36 + 3.62P - 0.099P^2, \\ C_{66} = 15.56 + 1.89P - 0.036P^2, \end{array} \right. \left\{ \begin{array}{l} C_{12} = 14.74 + 2.31P + 0.002P^2, \\ C_{13} = 28.91 + 4.39P - 0.028P^2, \\ C_{15} = -0.73 - 0.38P + 0.0079P^2, \\ C_{23} = 13.48 + 2.903P - 0.028P^2, \\ C_{25} = -2.87 - 0.091P - 0.024P^2, \\ C_{35} = -1.59 + 1.19P - 5.5 \times 10^{-3}P^2, \\ C_{46} = -3.23 - 0.03P - 0.012P^2. \end{array} \right. \quad (3.13)$$

### 3.2.2. Elastic constants for polycrystalline aggregates

The three pairs of isotropic elastic parameters such as bulk modulus  $B$  with the shear modulus  $G$  or the modulus of Young  $E$  with Poisson's ratio  $\delta$  or both Lamé's constants  $\lambda$  and  $\mu$  can be used to fully describe the mechanical behavior of a polycrystalline material.

The elastic constants  $C_{ijs}$  in our paper have been estimated from *ab initio* PP-PW calculations for Ba<sub>2</sub>P<sub>7</sub>X monocrystalline. These elastic constants  $C_{ij}$  of the single-crystal are used to obtain the isotropic elastic parameters. The mass modulus  $B$ , which measures the resistance of the solid to the volume changes under the applied hydrostatic pressure. The isotropic shear modulus  $G$  is a measure of resistance to reversible deformations caused by deformation. The shear strain can be determined experimentally on a polycrystalline sample to characterize its mechanical properties. Theoretically,  $B$  and  $G$  of the material's polycrystalline phase can be obtained from the appropriate average of the independent elastic constants  $C_{ijs}$  of its monocrystalline phase. The modulus of elasticity averaged by orientation  $B$  and  $G$  can be calculated using the Reuss-Voigt-Hill approximations [14, 15]. Here, the Voigt ( $B_V$ ,  $G_V$ ) and Reuss ( $B_R$ ,  $G_R$ ) approximations represent extreme values for  $B$  and  $G$ ; and are expressed as follows [25]:

$$\left\{ \begin{array}{l}
B_R = \Omega \left[ \begin{array}{l} a + (C_{11} + C_{22} - 2C_{12}) + b(2C_{12} - 2C_{11} - C_{23}) + c(C_{15} - 2C_{25}) + \\ d(2C_{12} + 2C_{23} - C_{13} - 2C_{22}) + 2e(C_{25} - C_{15}) + f \end{array} \right]^{-1}, \\
B_V = \frac{1}{9} [C_{11} + C_{22} + C_{33} + 2(C_{12} + C_{13} + C_{23})], \\
G_V = \frac{1}{15} [C_{11} + C_{22} + C_{33} + 3(C_{44} + C_{55} + C_{66}) - (C_{12} + C_{13} + C_{23})], \\
G_R = 15 \left\{ \frac{4[a(C_{11}+C_{22}+C_{12})+b(C_{11}-C_{12}-C_{23})+c(C_{15}+C_{25})+d(C_{22}-C_{12}-C_{23}-C_{13})+e(C_{15}-C_{25})+f]}{\Omega+3\left[\frac{g}{\Omega}+\left(\frac{C_{44}+C_{66}}{C_{44}C_{66}-C_{46}^2}\right)\right]} \right\}^{-1}, \\
\text{with :} \\
a = C_{33}C_{55} - C_{35}^2, \\
b = C_{23}C_{55} - C_{25}C_{35}, \\
c = C_{13}C_{35} - C_{15}C_{33}, \\
d = C_{13}C_{55} - C_{15}C_{35}, \\
e = C_{13}C_{25} - C_{15}C_{23}, \\
f = C_{11}(C_{22}C_{33} - C_{25}^2) - C_{12}(C_{12}C_{55} - C_{15}C_{25}) + C_{15}(C_{12}C_{25} - C_{15}C_{22}) + C_{25}(C_{23}C_{35} - C_{25}C_{33}), \\
g = C_{11}C_{22}C_{33} - C_{11}C_{23}^2 - C_{22}C_{13}^2 - C_{33}C_{12}^2 + 2C_{12}C_{13}C_{23}, \\
\Omega = \left\{ \begin{array}{l} 2[C_{15}C_{25}(C_{33}C_{12} - C_{13}C_{23}) + C_{15}C_{35}(C_{22}C_{13} - C_{12}C_{23}) + C_{25}C_{35}(C_{11}C_{23} - C_{12}C_{23})] - \\ [C_{15}^2(C_{22}C_{33} - C_{25}^2) + C_{25}^2(C_{11}C_{33} - C_{13}^2) + C_{35}^2(C_{11}C_{22} - C_{12}^2)] + gC_{55} \end{array} \right\}.
\end{array} \right. \quad (3.14)$$

Hill recommends that the arithmetic mean of these two limits (Voigt, Reuss) should be used in practice as an effective module for polycrystalline samples.

$$\left\{ \begin{array}{l} B_H = \frac{B_V+B_R}{2}, \\ G_H = \frac{G_V+G_R}{2}. \end{array} \right. \quad (3.15)$$

Where  $B_H$  and  $G_H$  are the shear modulus of the polycrystalline according to Hill approximation. The Young's modulus  $E$  and Poisson's ratio  $\delta$  for an isotropic material can be computed from the Hill's values of  $B_H$  and  $G_H$  using the following expressions,

$$\left\{ \begin{array}{l} E = \frac{9B_HG_H}{3B_H+G_H}, \\ \delta = \frac{3B_H-2G_H}{6B_H+2G_H}. \end{array} \right. \quad (3.16)$$

The calculated bulk modulus  $B_H$ , shear modulus  $G_H$ , Young's modulus  $E$  and Poisson's ratio  $\delta$  are quoted in table 4. The obtained results allow us to make the following conclusions:

(i) From tables 3 and 4, one can see that the value of the bulk modulus for  $Ba_2P_7X$  deduced from the single-crystal elastic constants  $C_{ijs}$  is in good agreement with those calculated from the third order polynomial  $P(V)$ , Birch-Murnaghan  $P(V)$  EOS, Vinet  $P(V)$  EOS, Murnaghan  $P(V)$  EOS, Birch-Murnaghan  $E(V)$  EOS and Murnaghan  $E(V)$  EOS fits (figure 3). This similarity may serve as an estimate of the reliability and accuracy of this theoretical estimation of the elastic constants for the monoclinic Zintl phase  $Ba_2P_7X$ . We can see that the bulk modulus of the considered material is quite small (lower than 50 GPa), and therefore, this material should be classified as a relatively soft material with high compressibility (higher than 0.02) [27].

(ii) The Young's modulus, which is defined to be the ratio of linear stress to linear strain, may give information as to the stiffness of the material. The Young's modulus of  $Ba_2P_7X$  was discovered to approximate 48 GPa in the same order of  $C_{11}$ ,  $C_{22}$  and  $C_{33}$  values, which indicates the relatively high resistance of this compound to uniaxial deformation (compression/traction); thus, these compounds show a rather low stiffness. The highest Young's modulus belongs to  $Ba_2P_7Cl$  compound. Therefore, this compound is harder than the other compounds.

(iii) The Poisson's ratio is the factor that measures the stability of a crystal against shear [28], defined as the ratio of transverse strain (normal to the applied stress) to the longitudinal strain (in the direction of the applied stress), is generally connected with the volume change in a solid during uniaxial deformation and provides more information on the characteristics of the bonding forces than any of the other elastic

constants [27, 29, 30]. If  $\delta$  is equal to 0.5, no volume change occurs, while if it is lower than 0.5, a large volume change is expected for any elastic deformation [31], and it has been proved that  $\delta = 0.25$  is the lower limit for central force and  $\delta = 0.5$  is the upper limit. In our case, the value of  $\delta$  is approximately 0.30 in Ba<sub>2</sub>P<sub>7</sub>X, suggesting that a considerable volume change can be associated with elastic deformation and that the interatomic forces in this compound are central.

(vi) The bulk and shear moduli provide information regarding the brittle-ductile nature of a material. Pugh [32] has proposed a simple empirical relationship between the bulk modulus  $B_H$  and shear modulus  $G_H$ . According to these criteria, the calculated value of  $B_H/G_H$  is higher than 1.75, which may be associated to the ductility; whereas a value lower than 1.75 is associated to brittleness. Based on Pugh's criteria, the three considered compounds Ba<sub>2</sub>P<sub>7</sub>X are ductile materials.

(v) The Debye temperature  $\theta_D$  is used to distinguish between high and low temperatures for a solid in the Debye model. The Debye temperature  $\theta_D$  is correlated with many physical properties, such as thermal expansion, melting point and Grüneisen parameter. The flow temperature  $\theta_D$  can be estimated numerically from the mean speed of the sound wave  $V_m$  as follows [33]:

$$\theta_D = \frac{h}{k_B} V_m \left[ \frac{3n N_A \rho}{4\pi M} \right]^{1/3}. \quad (3.17)$$

where,  $h$  is Planck constant,  $k_B$  is Boltzmann constant,  $N_A$  is Avogadro number,  $\rho$  is the mass density,  $M$  is the molecular weight and  $n$  is the number of atoms in the molecule. In polycrystalline materials, the average wave velocity  $V_m$  can be evaluated as follows [33]:

$$V_m = \left[ \frac{1}{3} (2V_T^{-3} + V_L^{-3}) \right]^{-1/3}. \quad (3.18)$$

Here,  $V_L$  and  $V_T$  are the average longitudinal and transverse elastic wave velocities, which are defined by Navier's equations [34]:

$$V_L = \left( \frac{3B + 4G}{3\rho} \right)^{1/2}, \quad (3.19)$$

$$V_T = \left( \frac{G}{\rho} \right)^{1/2}. \quad (3.20)$$

The results obtained for  $\theta_D$  and average sound velocities are listed in table 4. The sound velocity in the Ba<sub>2</sub>P<sub>7</sub>Cl compound is higher in the two compounds Ba<sub>2</sub>P<sub>7</sub>Br and Ba<sub>2</sub>P<sub>7</sub>I, like Debye temperatures ( $\theta_D$ ) values. Therefore, it can be said that the sound conductivity of Ba<sub>2</sub>P<sub>7</sub>Cl is better than that of other compounds.

From this table, it can be seen that Ba<sub>2</sub>P<sub>7</sub>X is characterized by a high Debye temperature equal to 260 K, the Debye temperature, the behavior of the sound velocity, the Young's modulus  $E$ , the Poisson's ratios  $\delta$  and the Pugh  $B_H/G_H$  ratio under the effect of pressure are shown in figure 5, this figure shows that all these physical parameters increase with an increase of the pressure and are well adjusted by a second order polynomial equation for the three compounds Ba<sub>2</sub>P<sub>7</sub>Cl, Ba<sub>2</sub>P<sub>7</sub>Br, Ba<sub>2</sub>P<sub>7</sub>I, respectively:

$$\begin{cases} \frac{B_H}{G_H} = 1.8 + 0.064P - 1.52 \times 10^{-3}P^2, \\ E = 48.08 + 4.94P - 0.093P^2, \\ \delta = 0.266 + 6.2 \times 10^{-3}P - 1.8 \times 10^{-4}P^2, \\ V_L = 4078.73 + 228.88P - 5.21P^2, \\ V_T = 2303.80 + 102.27P - 2.52P^2, \\ V_m = 2562.5 + 116.06P - 2.85P^2, \\ \theta_D = 262.93 + 11.91P - 0.293P^2, \end{cases} \quad (3.21)$$

**Table 4.** The calculated bulk modulus ( $B_H$ , in GPa); shear modulus ( $G_H$ , in GPa); Young's modulus ( $E$ , in GPa); Poisson's ratio ( $\delta$ ); mass density  $\rho$  ( $\text{g/cm}^3$ ); longitudinal, transverse and average sound velocities ( $V_L$ ,  $V_T$  and  $V_m$ , in m/s) and Debye temperature ( $\theta_D$ , in K). For the monoclinic Zintl phase  $\text{Ba}_2\text{P}_7\text{X}$ , it is obtained using the single-crystal elastic constants  $C_{ijs}$ . The subscript V, R or H indicates that the modulus was obtained using Voigt theory or Reuss theory and Hill theory, respectively.

System	$\rho$	$B_V$	$B_R$	$B_H$	$G_V$	$G_R$	$G_H$
$\text{Ba}_2\text{P}_7\text{Cl}$	3.58	34.22	33.80	34.01	19.44	18.26	18.85
$\text{Ba}_2\text{P}_7\text{Br}$	3.83	34.45	35.05	34.75	19.50	17.95	18.55
$\text{Ba}_2\text{P}_7\text{I}$	3.75	33.18	37.21	34.20	20.36	16.70	18.53
System	$B_H/G_H$	$E$	$\delta$	$V_L$	$V_T$	$V_m$	$\theta_D$
$\text{Ba}_2\text{P}_7\text{Cl}$	1.80	47.74	0.266	4064.91	2294.92	2552.66	262
$\text{Ba}_2\text{P}_7\text{Br}$	1.87	47.25	0.273	3941.31	2200.95	2450.31	250
$\text{Ba}_2\text{P}_7\text{I}$	1.89	47.30	0.276	3997.06	2149.86	2394.20	242

$$\left\{ \begin{array}{l} \frac{B_H}{G_H} = 1.86 + 0.0646P - 1.52 \times 10^{-3}P^2, \\ E = 47.65 + 5.07P - 0.09P^2, \\ \delta = 0.272 + 5.8 \times 10^{-3}P - 1.64 \times 10^{-4}P^2, \\ V_L = 3938.99 + 241.2P - 5.91P^2, \\ V_T = 2203.42 + 110.12P - 2.98P^2, \\ V_m = 2452.8 + 124.65P - 3.35P^2, \\ \theta_D = 250.55 + 12.73P - 0.34P^2, \end{array} \right. \quad (3.22)$$

$$\left\{ \begin{array}{l} \frac{B_H}{G_H} = 1.89 + 0.060P - 1.15 \times 10^{-3}P^2, \\ E = 47.44 + 5.43P - 0.11P^2, \\ \delta = 0.276 + 5.4 \times 10^{-3}P - 1.37 \times 10^{-4}P^2, \\ V_L = 3873.63 + 232.73P - 5.34P^2, \\ V_T = 2155.03 + 106.2P - 2.78P^2, \\ V_m = 2399.7 + 120.67P - 3.17P^2, \\ \theta_D = 242.45 + 12.13P - 0.315P^2. \end{array} \right. \quad (3.23)$$

### 3.2.3. Elastic anisotropy

The anisotropy of the physical properties in the crystals and a correct description of the anisotropic behavior, and the elastic anisotropy is another interesting physical parameter with respect to the elastic properties of the solids. It reflects the anisotropy in the bond between the atoms in different crystallographic directions. Anisotropic characters of binding and structural stability are usually defined by the elastic constants  $C_{ijs}$ . These constants have been often related to the shear modulus  $G$  and Young's modulus  $E$ . We have previously reported that the three  $\text{Ba}_2\text{P}_7\text{X}$  materials are anisotropic in terms of compressibility (figure 2). It is important to evaluate the elastic anisotropy of a solid to understand the micro cracks that are easily induced in materials due to a significant anisotropy of the coefficient of thermal expansion as well as the elastic anisotropy [29] and its influence on nanoscale precursor textures of alloys [35]. Different approaches were developed to describe the materials' elastic anisotropy. Four different criteria were employed to quantify the anisotropy of the elastic properties of the  $\text{Ba}_2\text{P}_7\text{Cl}$ ,  $\text{Ba}_2\text{P}_7\text{Br}$  and  $\text{Ba}_2\text{P}_7\text{I}$  compounds.

- (i) A method of measuring the elastic anisotropy which consists in considering the percentage of

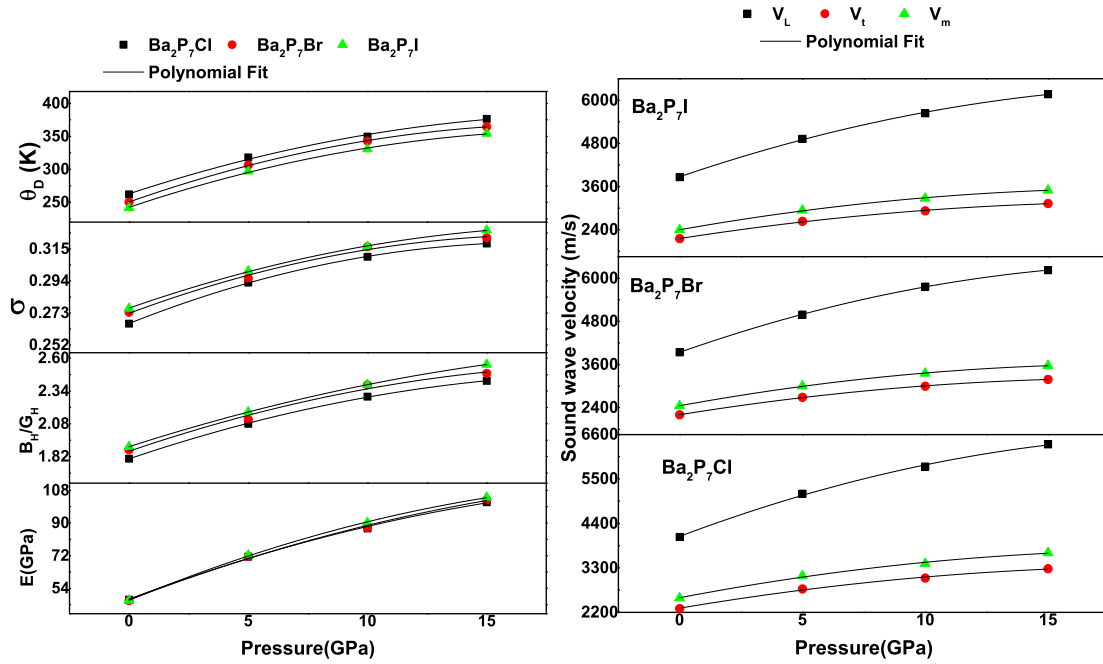


**Figure 5.** (Colour online) The calculated pressure dependence of Pugh's ratio  $B_H/G_H$ , Young's modulus  $E$ , Poisson's ratio  $\delta$ , Debye temperature  $\theta_D$ , and the isotropic sound velocity (longitudinal  $V_L$ , transverse  $V_T$  and average  $V_m$ ) for the monoclinic Zintl phase Ba<sub>2</sub>P<sub>7</sub>X. The symbols indicate the calculated results. The lines represent the results of fitting these theoretical results to a second-order polynomial.

anisotropy in the compression and shear modulus was proposed by Chung and Buessem [36]:

$$\begin{cases} A_B = \frac{B_V - B_R}{B_V + B_R} \times 100, \\ A_G = \frac{G_V - G_R}{G_V + G_R} \times 100, \end{cases} \quad (3.24)$$

where  $B$  and  $G$  are the bulk and shear moduli, respectively, and the subscripts V and R represent the Voigt and Reuss bounds, a value of zero (0 %) represents elastic isotropy and a value of (100 %) represents the largest possible elastic anisotropy. The results shown in table 5 for  $A_B$  and  $A_G$  suggest that Ba<sub>2</sub>P<sub>7</sub>Cl, Ba<sub>2</sub>P<sub>7</sub>Br and Ba<sub>2</sub>P<sub>7</sub>I compounds are anisotropic.

(ii) A universal anisotropy index  $A^U$  was proposed by Ranganathan and Ostoja-Starzewski [37] to quantify the elastic anisotropy of three crystals accounting for bulk and shear modulus contributions. The index  $A^U$  is delimited as follows:

$$A^U = 5 \frac{G_V}{G_R} + \frac{B_V}{B_R} - 6. \quad (3.25)$$

For isotropic crystals, the universal index is equal to zero ( $A^U = 0$ ); the deviation of  $A^U$  from zero defines the extent of the anisotropy of a crystal. The results listed in table 5 for  $A^U$  indicate that Ba<sub>2</sub>P<sub>7</sub>Cl, Ba<sub>2</sub>P<sub>7</sub>Br and Ba<sub>2</sub>P<sub>7</sub>I have a certain degree of elastic anisotropy.

**Table 5.** The calculated percentage of elastic anisotropy for bulk modulus and shear modulus ( $A_B$  and  $A_G$ ) and universal anisotropy index ( $A^U$ ) for the Ba<sub>2</sub>P<sub>7</sub>Cl, Ba<sub>2</sub>P<sub>7</sub>Br and Ba<sub>2</sub>P<sub>7</sub>I compounds.

System	$A_B$ %	$A_G$ %	$A^U$ %
Ba <sub>2</sub> P <sub>7</sub> Cl	0.61	3.12	0.33
Ba <sub>2</sub> P <sub>7</sub> Br	0.85	10.86	0.52
Ba <sub>2</sub> P <sub>7</sub> I	5.73	9.85	0.98

## 4. Conclusions

In this paper, a prediction of some physical properties of the monoclinic Zintl phase  $\text{Ba}_2\text{P}_7\text{X}$  ( $\text{X}=\text{Cl}, \text{Br}, \text{I}$ ) was obtained by using the PP-PW method based on DFT with the GGA PBEsol approach. At first, an accurate geometrical optimization was performed on the crystal structure, and then the structural and elastic properties of the three materials  $\text{Ba}_2\text{P}_7\text{Cl}$ ,  $\text{Ba}_2\text{P}_7\text{Br}$  and  $\text{Ba}_2\text{P}_7\text{I}$  were calculated in detail respectively. The results show that:

- The theoretically predicted lattice parameters for  $\text{Ba}_2\text{P}_7\text{Cl}$ ,  $\text{Ba}_2\text{P}_7\text{Br}$  and  $\text{Ba}_2\text{P}_7\text{I}$  are in good agreement with the existing experimental measurements. The calculated zero-pressure single-crystal elastic constants  $C_{ij}$  of  $\text{Ba}_2\text{P}_7\text{X}$  ( $\text{X}=\text{Cl}, \text{Br}, \text{I}$ ) satisfy the dynamical stability criteria.
- The pressure dependence of the elastic constants reveals that  $\text{Ba}_2\text{P}_7\text{X}$  ( $\text{X}=\text{Cl}, \text{Br}, \text{I}$ ) remains mechanically stable under hydrostatic pressure effect as well.
- This paper calculates and estimates the elastic constants, and other related quantities consisting in Young's modulus, shear modulus, Poisson's ratio, anisotropy factor, sound velocities, and Debye temperature.
- The material has a relatively small bulk modulus and a brittle character. The bulk modulus derived from the single-crystal elastic constants  $C_{ij}$  is observed to be in excellent agreement with the one estimated from the EOS-fitting. This result shows the reliability of our calculations.
- The investigated properties demonstrate that the three compounds are relatively soft materials.
- The elastic constants of three single-crystal and polycrystalline phases of  $\text{Ba}_2\text{P}_7\text{X}$  were estimated. The  $\text{Ba}_2\text{P}_7\text{X}$  compounds exhibit a noticeable elastic anisotropy. And finally, by using the empirical rule of Pugh, the  $B/G$  ratio, we have demonstrated that the studied compound should be classified as a relatively ductile material.

## Acknowledgements

The authors would like to thank Dr. Zitouni H., Dr. Ahmed Ammar M., Mr. Media M. and Mr. Houatis D. for their, help, support, and constant assistance and for their advice throughout this project.

## References

1. Dolyniuk J.-A., Kovnir K., *Crystals*, 2013, **3**, 431–442, doi:10.3390/cryst3030431.
2. Eschen M., Jeitschko W., *J. Solid State Chem.*, 2002, **165**, 238–246, doi:10.1006/jssc.2001.9497.
3. Kraus F., Korber N., *Chem. Eur. J.*, 2005, **11**, 5945–5959, doi:10.1002/chem.200500414.
4. Dell S., Vogelaar N.J., Ho D.M., Pascal R.A., *J. Am. Chem. Soc.*, 1998, **120**, 6421–6422, doi:10.1021/ja981009s.
5. Miller G.J., Schmidt M.W., Wang F., You T.-S., In: *Zintl Phases. Structure and Bonding*, Vol. 139, Fässler T. (Ed.), Springer, Berlin, Heidelberg, 2011, 1–55, doi:10.1007/430\_2010\_24.
6. Manriquez V., Hönle W., von Schnering H.G., *Z. Anorg. Allg. Chem.*, 1986, **539**, 95–109, doi:10.1002/zaac.19865390810.
7. Dahlmann W., von Schnering H.G., *Naturwissenschaften*, 1973, **60**, 518, doi:10.1007/BF00603256.
8. Sin'ko G.V., *Phys. Rev. B*, 2008, **77**, 104118, doi:10.1103/PhysRevB.77.104118.
9. Zhijiao Z., Feng W., Zhou Z., Jianjun W., Xinyou A., Guo L., Weiyi R., *Physica B*, 2011, **406**, 737, doi:10.1016/j.physb.2010.11.040.
10. Clark S.J., Segall M.D., Pickard C.J., Hasnip P.J., Probert M.J., Refson K., Payne M.C., *Z. Kristallogr.*, 2005, **220**, 567, doi:10.1524/zkri.220.5.567.65075.
11. Perdew J.P., Ruzsinszky A., Csonka G.I., Vydrov O.A., Scuseria G.E., Constantin L.A., Zhou X., Burke K., *Phys. Rev. Lett.*, 2008, **100**, 136406, doi:10.1103/PhysRevLett.100.136406.
12. Vanderbilt D., *Phys. Rev. B*, 1990, **41**, 7892(R), doi:10.1103/PhysRevB.41.7892.
13. Monkhorst H.J., Pack J.D., *Phys. Rev. B*, 1976, **13**, 5188, doi:10.1103/PhysRevB.13.5188.
14. Voigt W., *Lehrbuch der Kristallphysik (Textbook of Crystal Physics)*, Teubner, Leipzig, 1928.
15. Hill R., *Proc. Phys. Soc. London, Sect. A*, 1952, **65**, 349–354, doi:10.1088/0370-1298/65/5/307.
16. Schnering H.G.V., Menge G., *Z. Anorg. Allg. Chem.*, 1981, **481**, 33–40, doi:10.1002/zaac.19814811005.

17. Wu M.-M., Wen L., Tang B.-Y., Peng L.-M., Ding W.-J., *J. Alloys Compd.*, 2010, **506**, 412, doi:10.1016/j.jallcom.2010.07.018.
18. Ambrosch-Draxl C., Sofo J.O., *Comput. Phys. Commun.*, 2006, **175**, 1–14, doi:10.1016/j.cpc.2006.03.005.
19. Hebbache M., Zenzemi M., *Phys. Rev. B*, 2004, **70**, 224107, doi:10.1103/PhysRevB.70.224107.
20. Birch F., *J. Geophys. Res.*, 1978, **83**, 1257–1268, doi:10.1029/JB083iB03p01257.
21. Fu C.-L., Ho K.-M., *Phys. Rev. B*, 1983, **28**, 5480, doi:10.1103/PhysRevB.28.5480.
22. Murnaghan F.D., *Proc. Natl. Acad. Sci. U.S.A.*, 1944, **30**, 244–247, doi:10.1073/pnas.30.9.244.
23. Birch F., *Phys. Rev.*, 1947, **71**, 809, doi:10.1103/PhysRev.71.809.
24. Westbrook J.H., Fleischer R.L., John Wiley & Sons Ltd, Baffins Lane, Chichester, West Sussex PO 19 1UD, England, 2000.
25. Wu Z.-J., Zhao E.-J., Xiang H.-P., Hao X.-F., Liu X.-J., Meng J., *Phys. Rev. B*, 2007, **76**, 054115, doi:10.1103/PhysRevB.76.054115.
26. Sin'ko G.V., Smirnov N.A., *J. Phys.: Condens. Matter*, 2002, **14**, 6989, doi:10.1088/0953-8984/14/29/301.
27. Haddadi K., Bouhemadou A., Louail L., *Solid State Commun.*, 2010, **150**, 932–937, doi:10.1016/j.ssc.2010.02.024.
28. Guechi N., Bouhemadou A., Khenata R., Bin-Omran S., Chegaar M., Al-Douri Y., Bourzami A., *Solid State Sci.*, 2014, **29**, 12–23, doi:10.1016/j.solidstatesciences.2014.01.001.
29. Ravindran P., Fast L., Korzhavyi P.A., Johansson B., *J. Appl. Phys.*, 1998, **84**, 4891, doi:10.1063/1.368733.
30. Bouhemadou A., Uğur G., Uğur Ş., Al-Essa S., Ghebouli M.A., Khenata R., Bin-Omran S., Al-Dour Y., *Comput. Mater. Sci.*, 2013, **70**, 107–113, doi:10.1016/j.commatsci.2013.01.004.
31. Appalakondaiah S., Vaitheeswaram G., Lebègue S., Christensen N.E., Svane A., *Phys. Rev. B*, 2012, **86**, 035105, doi:10.1103/PhysRevB.86.035105.
32. Pugh S.F., *Philos. Mag.*, 1954, **45**, 823–843, doi:10.1080/14786440808520496.
33. Anderson O.L., *J. Phys. Chem. Solids*, 1963, **24**, 909–917, doi:10.1016/0022-3697(63)90067-2.
34. Schreiber E., Anderson O.L., Soga N., *Elastic Constants and Their Measurements*, McGraw-Hill Companies, New York, 1974.
35. Lloveras P., Castán T., Porta M., Planes A., Saxena A., *Phys. Rev. Lett.*, 2008, **100**, 165707, doi:10.1103/PhysRevLett.100.165707.
36. Chung D.H., Buessem W.R., In: *Anisotropy in Single-Crystal Refractory Compounds*, Vol. 2, Vahldiek F.W., Mersol S.A. (Eds.), Plenum, New York, 1968, 217–246, doi:10.1007/978-1-4899-5307-0.
37. Ranganathan S.I., Ostoja-Starzewski M., *Phys. Rev. Lett.*, 2008, **101**, 055504, doi:10.1103/PhysRevLett.101.055504.

## Дослідження структурних та пружних властивостей моноклінних $Ba_2P_7X$ ( $X = Cl, Br, I$ ) солей Цінтля

М. Раджай<sup>1,2</sup>, Д. Мауш<sup>1</sup>, Н. Гуеші<sup>3</sup>, С. Шеддаді<sup>4</sup>, З. Кешіді<sup>5</sup>

<sup>1</sup> Лабораторія для отримання нових матеріалів і їхня характеристика, університет Ферхат Аббас Сетіф 1, Алжир

<sup>2</sup> Лабораторія фізики експериментальних методик та їх застосування (LPTEAM), університет м. Медеа, Алжир

<sup>3</sup> Лабораторія досліджень поверхонь та інтерфейсів твердих матеріалів, університет Ферхат Аббас Сетіф 1, Алжир

<sup>4</sup> Лабораторія радіаційної фізики, фізичний відділ, факультет природничих наук, університет Ваджі Мохтар, Аннаба, Алжир

<sup>5</sup> Лабораторія електротехніки та автоматики LREA, університет м. Медеа, Алжир

Досліджувалися структурні і пружні властивості  $Ba_2P_7X$  ( $X=Cl, Br, I$ ) сполук Цінтля, використовуючи метод псевдопотенціальної плоскої хвилі (PP-PW), що базується на теорії функціоналу густини (DFT) в межах узагальненого градієнтного наближення (GGA-PBESOL). Розраховані сталі ґратки і внутрішні параметри добре узгоджуються з експериментальними результатами, відомими з літератури. В цій статті ми представляємо дослідження відносних змін структурних параметрів і пружних констант як функцій гідростатичного тиску. Ізотропні модулі пружності та пов'язані з ними властивості для монокристала і полікристалічної фази, включаючи, зокрема, об'ємні модулі, зсувні модулі, модулі Юнга, коефіцієнт Пуассона, пружні анізотропні індекси, індикатор Пуга поведінки крихкість/пластичність, швидкості пружної хвилі і температура Дебая були оцінені з  $C_{ij}$ , використовуючи наближення Войгта, Реусса і Хілла. Два різні методи були використані для вивчення пружної анізотропії цих сполук.

**Ключові слова:** сполука Цінтля,  $P_7^{-3}$  кластери, модуль пружності, *ab initio* обчислення